Journal of Thermal Science Vol.19, No.2 (2010) 120−125

DOI: 10.1007/s11630-010-0120-7 **Article ID: 1003-2169(2010)02-0120-06**

Acoustic Noise from Tandem Wind Rotors of Intelligent Wind Power Unit

Koichi Kubo, Nobuhiko Mihara, Akira Enishi and Toshiaki Kanemoto

Kyushu Institute of Technology: Sensui 1-1, Tobata, Kitakyushu, Fukuoka, 804-8550 Japan

The authors had invented the unique wind power unit composed of the large-sized front wind rotor, the small-sized rear wind rotor and the peculiar generator with the inner and the outer rotational armatures without the conventional stator. This unit is called "Intelligent Wind Power Unit" by the authors. The front and the rear wind rotors drive the inner and the outer armatures, respectively, while the rotational torque is counter-balanced between both armatures/wind rotors. This paper discusses experimentally the acoustic noise from the front and the rear wind rotors. The acoustic noise, in the counter-rotating operation, is induced mainly from the flow interaction between both rotors, and has the dominant power spectrum density at the frequency of the blade passing interaction. The noise is caused mainly from the turbulent fluctuation due to the flow separation on the blade, when the rear wind rotor stops or rotates in the same direction as the front wind rotor.

Keywords: Acoustic noise, Wind turbine, Tandem wind rotors, Counter-rotation

Introduction

Wind energy is clean, renewable and homegrown energy resources for electric power generations, and has been positively/effectively utilized to cope with the global warming environment. The authors had invented the superior wind power unit [1], as shown in Fig. 1. This unit is composed of the large-sized front wind rotor, the small-sized rear wind rotor and the peculiar generator with the inner and the outer armatures without the conventional stator. This unit is called "Intelligent Wind Power Unit" by the authors. The superior operation of this unit was verified in the previous report [1]-[3]. That is, the rotational torque is counter balanced between the inner and the outer armatures of the generator. The rotational directions and the speeds of both wind rotors/armatures are free, and automatically adjusted pretty well in response to the wind circumstances.

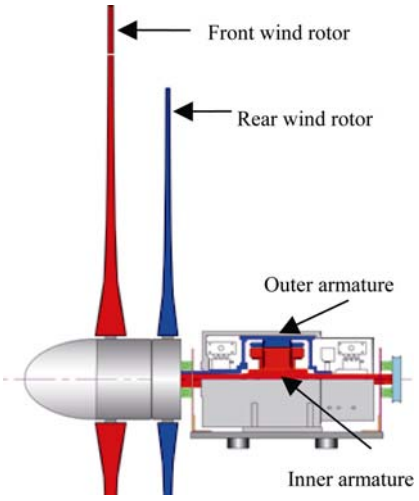

Fig. 1 Intelligent Wind Power Unit

Both wind rotors start to rotate at the cut-in wind velocity, but the rear wind rotor counter-rotates against the front wind rotor, as shown in Fig. 2. Both wind rotor speeds increase with the increase of the wind velocity,

Received: October 2009
Koichi Kubo:

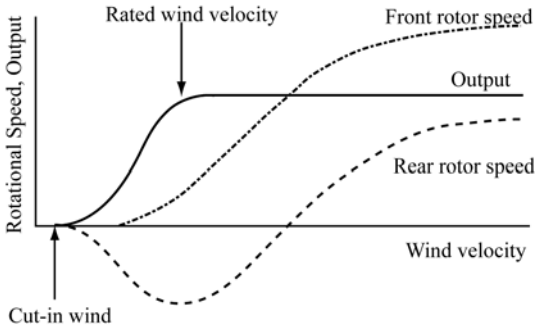

Fig. 2 Operation of Intelligent wind power unit

and the rear wind rotor reaches the maximum speed at the rated wind velocity.

With more increment of the wind velocity, the rotational speed of the rear wind rotor decreases gradually, stops, and begins to rotate in the same direction as the front wind rotor. Such superior operations of the tandem wind rotors may make the unacceptable acoustic noise, as compared with the traditional type wind turbines. This paper discusses experimentally the acoustic noise from tandem wind rotors, at the unique rotational conditions as mentioned before.

Model Wind Rotors and Experiments

To reduce the background noise as possible, the model wind rotors were set at the outlet of the wind tunnel (the nozzle diameter is 320 mm) which were covered by the anechoic box, as shown in Fig. 3. The blade profiles of both wind rotors are shown in Fig. 4, and are similar to the profiles in the performance tests, namely Front and Rear Blade G [4]. These sectional elements are MEL002 and are twisted to get the desirable attack angles irrespective of the radial position. The front and the rear blade setting angles, measured from the tangential direction at the tip (see Fig. 5), are β_F=5 degrees and β_R=15 degrees. The diameter ratio between both wind rotors is D_{RF} = (the rear wind rotor: d_R) / (the front wind rotor: d_F) = 0.84. The blade numbers of the front and the rear wind rotors are 3 and 5. These dimensions were also optimized at the previous report [4].

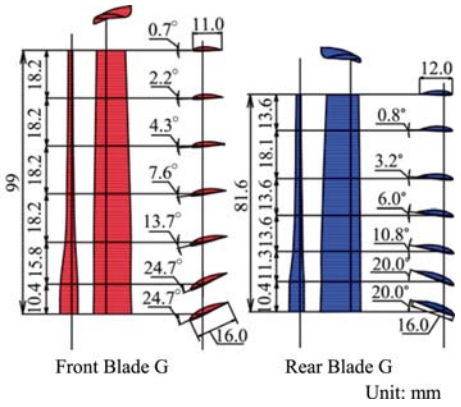

Fig. 4 Blade profiles of tandem wind rotors

The axial distance l between both wind rotors was changed from $L = l/d_F$ = 0.08 to 0.18, where d_F is the diameter of the front wind rotor (=230 mm). The front and the rear wind rotors were connected directly and respectively to the isolated motor with the inverter, in place of the peculiar generator described before.

In the experiments, the rotational speeds of both wind rotors were adjusted reasonably in accordance with the performance test [4], while the wind velocity was kept constant V=9m/s with the Reynolds number Re=$l_C\, w_{FT} / \nu$ = 1.3 ~ 3.9 x 10^5(l_C and w_{FT}: the chord and the relative velocity at the front blade tip). The absolute acoustic noises and the flow conditions differ more or less from those in the prototype, owing to the smaller Re number. The general circumstances of the acoustic noise, however, can be known in the experiments because the flow from

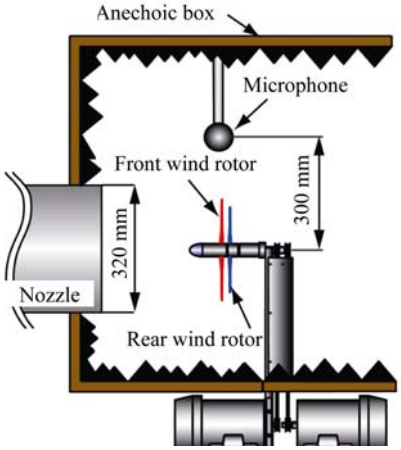

Fig. 3 Experimental setup

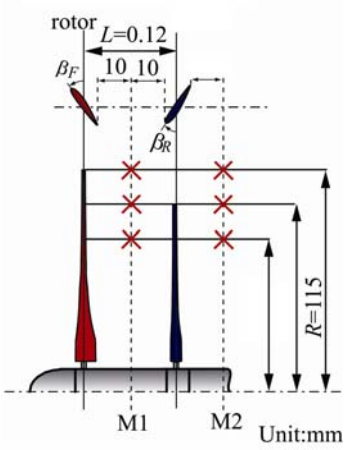

Fig. 5 Flow measurement points

the wind tunnel has higher velocity fluctuations and that promotes the transition from the laminar to the turbulent boundary layers. The microphone of the sound-level meter was set at the position of 300 mm in the radial direction measured from the center of hub, on the rotational plane of the front wind rotor. The output signal from the sound-level meter was accumulated in a FFT analyzer. The level and the frequency of the acoustic noise were evaluated without the background noises. The flow around the tandem wind rotors was measured by a hot wire anemometer. Figure 5 shows the measurement points.

Acoustic Noise at Counter-Rotation

Noise at the maximum output operation

Figure 6 shows the output coefficient C_P of the tandem wind rotors at the counter-rotation in the performance tests [4]. The maximum output is obtained at the relative tip speed ratio λ_T= (relative tip speed) / (wind velocity) = 5.58, while the ratio of the front and the rear wind rotors are λ_F = 3.12 and λ_R = 2.04, respectively, where the rotational speeds if the front and the rear wind rotors are N_F=2330 min^{-1}, N_R=-1844 min^{-1}. Figure 7 shows the power spectrum density of the acoustic noise at the maximum output operation (λ_T=5.58), where the blade passing frequencies are N_FZ_F=117 Hz for the front wind rotor and N_RZ_R=154 Hz for the rear wind rotor, and $L_{Aeq,T}$ = 64.1 dB gives the equivalent continuous A-weighted sound pressure level. These frequencies are hardly observed, but there are many dominant frequencies which may be attributed to the flow interaction between the front and the rear wind rotors. Hanson has predicted the dominant frequency in the counter-rotating propellers. That is, the dominant frequency f due to the flow interaction can be obtained from $f = |mZ_FN_F + kZ_RN_R|$, where m and k are the integral values (-∞~∞) giving the harmonic frequencies of N_FZ_F and N_RZ_R. Table 1(a) shows the dominant frequencies at λ_T= 5.58 derived from the above equation. These values coincide well with the experiments shown in Fig. 7.

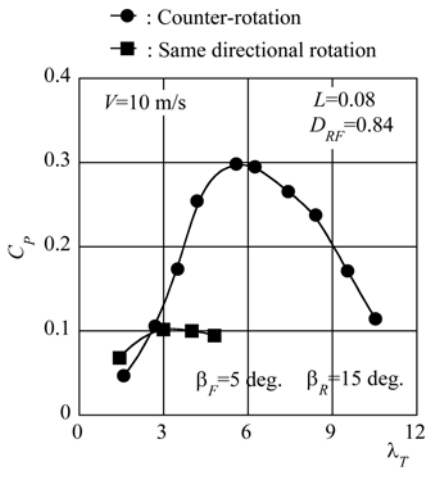

Fig. 6 Output of the tandem wind rotors

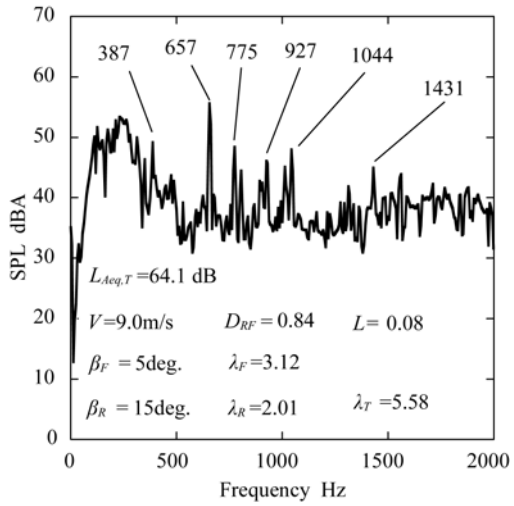

Fig. 7 The power spectrum density at λ_T=5.58

Effect of the axial distance between both wind rotors

Figure 8 shows the effect of the axial distance $L=l/d_F$ between the front and the rear wind rotors on the sound pressure level $L_{Aeq,T}$ at λ_T = 5.58. The level $L_{Aeq,T}$ at L=0.08 is 3.3 dB higher than one at L=0.18. That is, the tandem wind rotors make the unacceptable acoustic noise owing to the flow interaction. This result means that the longer distance L is acceptable as for the acoustic noise, but the shorter distance is acceptable as for the output [4].

Figure 9 shows the power spectrum densities at L=0.08 and 0.18. Some dominant frequencies appear obviously at L=0.08 where the rear wind rotor is close to the front wind rotor.

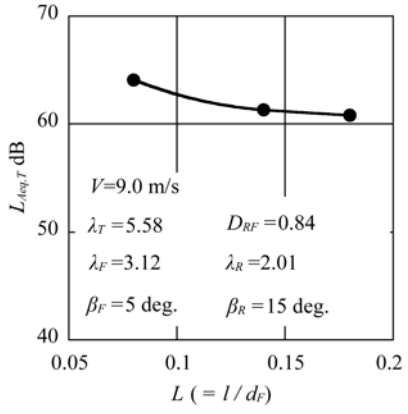

Fig. 8 Effect of axial distance between both wind rotors on the $L_{Aeq,T}$

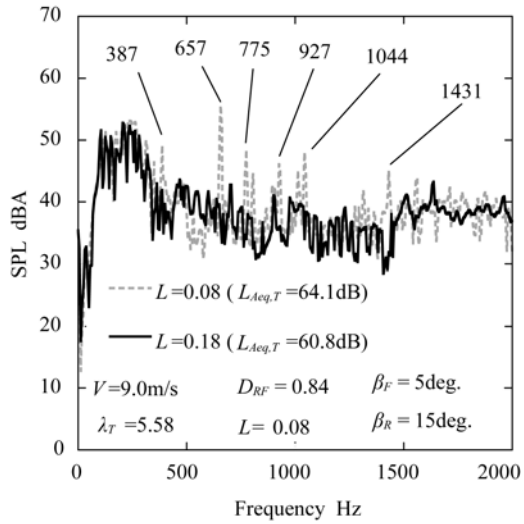

Fig. 9 The power spectrum density at L=0.08 and L=0.18

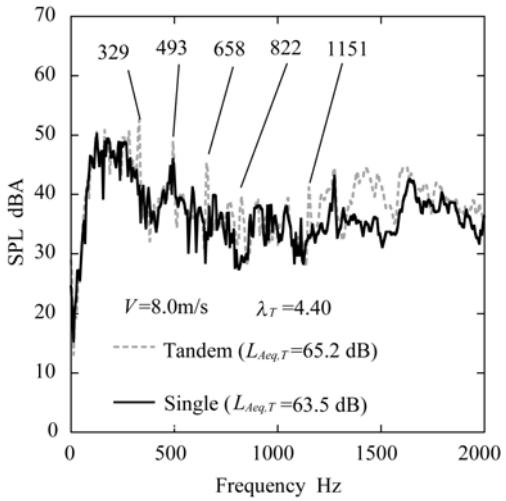

Fig. 10 The power spectrum density comparison with single rotor

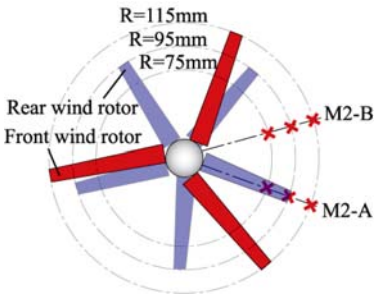

Fig. 11 Measurement sections M2-A and M2-B

Acoustic Noise at Rear Wind Rotor Stop

Figure 10 shows the power spectrum density and the sound pressure level $L_{Aeq,T}$ of the tandem wind rotors but the rear wind rotor stops, in comparison with these of the front wind rotor without the rear wind rotor which is called here the single wind rotor. The density of the tandem wind rotors is obviously higher than one of the single wind rotor in the wideband frequency from 1200 to 1600 Hz. That may be induced from the turbulent velocity fluctuations in the wake flow from the stopped rear blade with large scaled stall. Besides, the blade passing ($N_F Z_F$=164.4Hz) and the harmonic frequencies appeared obviously as compare with the single wind rotor, because of the flow interaction between both rotors.

The axial velocity components V_M measured by the hot wire anemometer are shown in Fig. 12, where M2-A is at the position just behind the rear blade and M2-B is at the middle position between rear blade cascade, as shown in Fig. 11. The flow conditions at Section M2-A verify that the turbulent velocity fluctuations are very large in the wake flow. On the contrary, the velocities scarcely fluctuate in the region smaller than the radius of the rear wind rotor at Section M2-B in the main flow. At R = 115 mm, the shed vortex from the front blade may make the downstream fluctuate and the flow condition around the tandem wind rotors is almost the same as the condition around the single wind rotor.

Acoustic Noise at Same Directional Rotation

Figure 13 shows the effect of the relative rotational speed on the acoustic noise while the rear wind rotor rotates in the same direction as the front wind rotor, where the output coefficient is maximum at λ_T=3.99 as shown in Fig. 6. Some dominant frequencies appear as shown in Figs. 7 and 9, even if the rear wind rotor rotates in the same direction as the front wind rotor. The density at the wideband frequency 1200~1900Hz is higher than that shown in Fig. 10, because the rear blade rotating in the blowing mode has the large attack angle and the large scaled stall as compared with the blade stopping. Besides, the sound pressure level and density increase with the increase of the relative tip speed ratio λ_T.

Figure 14 shows the axial velocity V_M fluctuations at λ_T=1.43 and 3.99 on section M2. The velocity becomes to fluctuate markedly with the decrease of the relative tip speed ratio λ_T, because of the wake flow described above.

Concluding Remarks

The acoustic noise from the tandem wind rotors was investigated at the representative operating conditions of Intelligent Wind Power Unit. The noise, in the counter-rotating operation, is induced mainly from the flow interaction between the front and the rear wind rotors, and has the dominant power spectrum density at the fre-

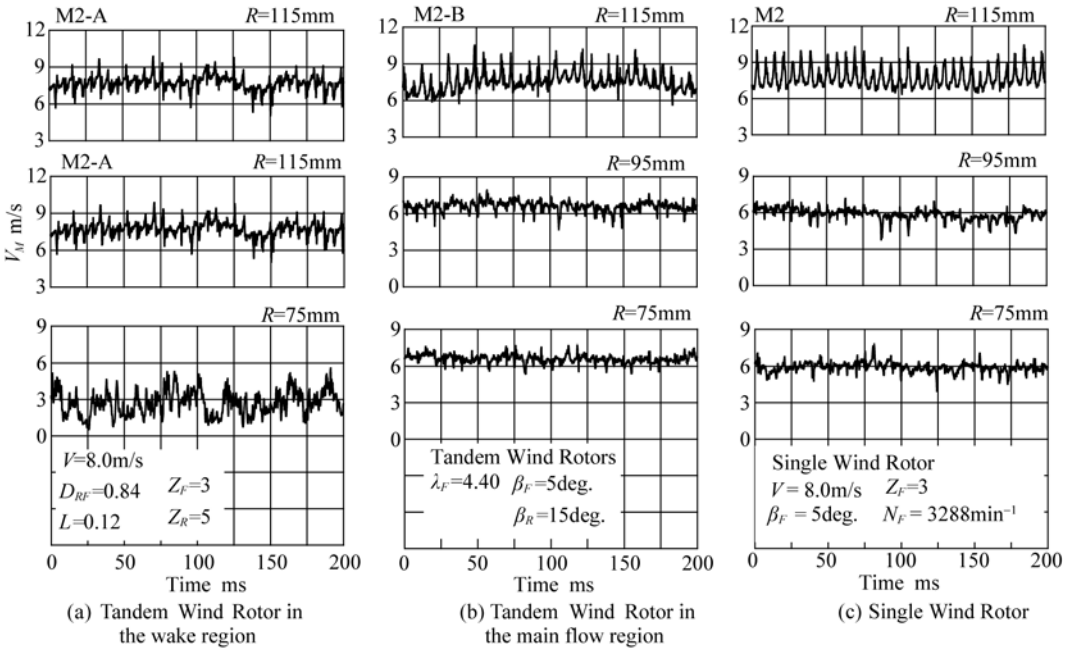

Fig. 12 Axial velocity fluctuations at Section M2

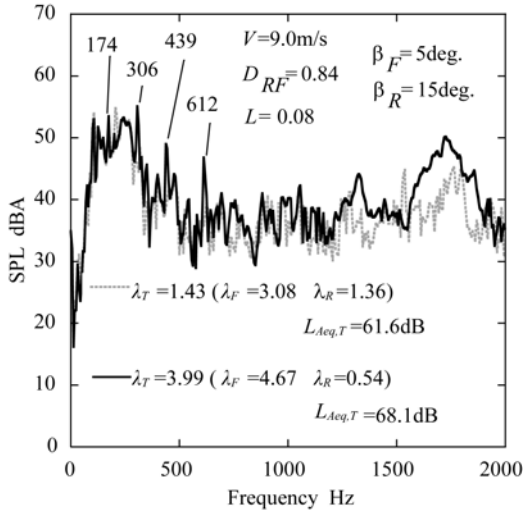

Fig. 13 The power spectrum density at λ_T=1.43 and λ_T=3.99

quency of the blade passing interaction. The noise is caused mainly from the turbulent fluctuation due to the flow separation on the blade, when the rear wind rotor stops or rotates in the same direction as the front wind rotor.

Acknowledgement

The authors wish to thank Mr. Yohei Hano being student of Graduate School of Engineering, Kyushu Institute of Technology, for helping the experiments. Some parts of this research were co-sponsored by Research Project 2007 "Grand-in-aid for Scientific Research (c) (2) in Japan" and Research project: Grant-in-aid for JSPS fellow.

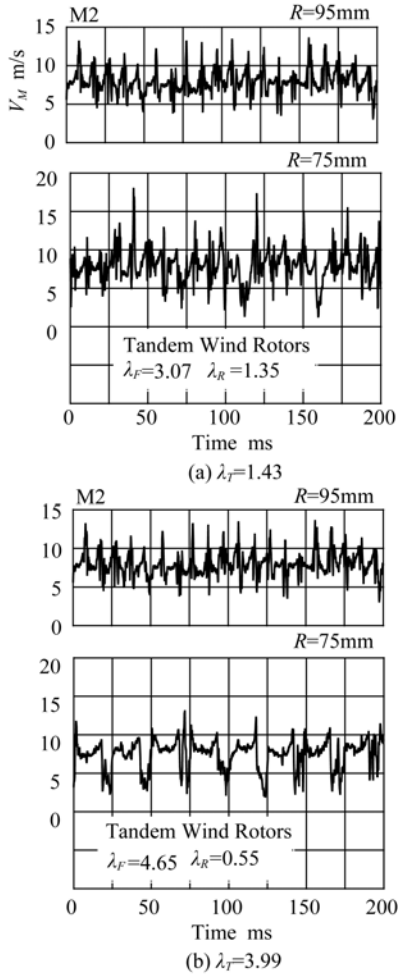

Fig. 14 Axial velocity fluctuations at λ_T=1.43 and λ_T=3.99

References

[1] Kanemoto, T. et al., “Intelligent Wind Turbine Generator with Tandem Rotors Applicable to Offshore Wind Farm”, Proceedings of the 15th International Offshore and Polar Engineering Conference and Exhibition, Vol.1, Seoul, Korea, 2005, pp.457–462 & Patent Nos. 4040939 and pending.

[2] Kanemoto, T. and Ahmed Mohamed GALAL, “Development of Intelligent Wind Turbine Generator with Tandem Wind Rotors and Double Rotational Armatures (1st Report, Superior Operation of Tandem Wind Rotors)”, JSME International Journal, Series B, Vol.49, No.2, 2006, pp.450–457

[3] Kanemoto, T. et al., “Intelligent wind turbine generator with tandem rotors applicable to offshore wind farm (characteristics of the peculiar generator and the performance of three dimensional blades)”, Proceedings of the 17th International offshore and polar engineering conference, Lisbon, 2007, pp.363–368

[4] Kubo, K. and Kanemoto, T, “Development of Intelligent Wind Turbine Unit with Tandem Wind Rotors and Double Rotational Armatures (2nd Report, Characteristics of tandem wind rotors)”, Journal of Fluid Science and Technology, Vol.3(2008), No.3, pp,370–378

[5] Hanson, D.B., “Noise of Counter-rotation Propellers”, J.Aircraft, 22(1985), p.609